

# Orbital differentiation and the role of orbital ordering in the magnetic state of Fe superconductors

E. Bascones,<sup>\*</sup> B. Valenzuela,<sup>†</sup> and M.J. Calderón<sup>‡</sup>

*Instituto de Ciencia de Materiales de Madrid, ICM-CONIC, Cantoblanco, E-28049 Madrid (Spain).*

(Dated: November 18, 2018)

We analyze the metallic  $(\pi, 0)$  antiferromagnetic state of a five-orbital model for iron superconductors. We find that with increasing interactions the system does not evolve trivially from the pure itinerant to the pure localized regime. Instead we find a region with a strong orbital differentiation between  $xy$  and  $yz$ , which are half-filled gapped states at the Fermi level, and itinerant  $zx$ ,  $3z^2 - r^2$  and  $x^2 - y^2$ . We argue that orbital ordering between the  $yz$  and  $zx$  orbitals arises as a consequence of the interplay of the exchange energy in the antiferromagnetic  $x$  direction and the kinetic energy gained by the itinerant orbitals along the ferromagnetic  $y$  direction with an overall dominance of the kinetic energy gain. We indicate that iron superconductors may be close to the boundary between the itinerant and the orbital differentiated regimes and that it could be possible to cross this boundary with doping.

PACS numbers: 75.10.Jm, 75.10.Lp, 75.30.Ds

There is a strong interrelation between the orbital degree of freedom, the magnetization, and the lattice structure in the Fe-superconductors. Unveiling the nature of these connections would define the landscape from which superconductivity emerges in these materials. One of the important issues is the determination of the strength of the interactions. Unlike the cuprates, which are antiferromagnetic Mott insulators when undoped, the Fe-superconductors are antiferromagnetic metals, highlighting the relevance of the itinerancy of the conduction electrons. Undoped materials have to accommodate six electrons in the five Fe-d orbitals, with an average filling of 1.2, close to the one of doped Mott insulators.<sup>1-3</sup> The itinerant<sup>4-7</sup> versus localized<sup>8,9</sup> origin of the magnetization has been discussed since the discovery of superconductivity in these systems.

On the other hand there is increasing evidence for orbital differentiation and a possible coexistence of itinerant and localized electrons.<sup>10-13</sup> Angle Resolved Photoemission Spectroscopy (ARPES) measurements report different renormalization values for the various bands close to the Fermi energy depending on their orbital character.<sup>14,15</sup> Similar qualitative conclusions may be inferred from Dynamical Mean Field Theory (DMFT) and slave-spin calculations.<sup>1,16-18</sup>

The possible role of orbital ordering in the magnetism is of present interest. The current debate is focused on whether it is the leading instability driving the magnetism<sup>19</sup> or it appears as a consequence of the magnetic ordering,<sup>20-23</sup> as well as its possible relation to the observed anisotropic properties.<sup>17,24-36</sup> In particular, the resistivity in the  $(\pi, 0)$  antiferromagnetic state was measured to be larger in the ferromagnetic  $y$ -direction than in the antiferromagnetic  $x$ -direction<sup>24,25</sup> with a change in sign upon hole doping.<sup>37</sup>

In order to shed light on the role of the different orbitals on the magnetic state of Fe-superconductors, we analyze the metallic  $(\pi, 0)$  antiferromagnetic state as a function of the interactions treated within mean-field.

Close to the non-magnetic phase boundary, electrons are itinerant. An  $S = 2$  state compatible with a localized  $J_1 - J_2$  description is found deep in the insulating regime.<sup>22</sup> With increasing interactions the system does not evolve trivially from the pure itinerant to the pure localized regime. Instead we find a region with a strong orbital differentiation, see Fig. 1. In this region,  $zx$ ,  $3z^2 - r^2$  and  $x^2 - y^2$  are itinerant while  $xy$  and  $yz$  are half-filled and have a gap at the Fermi level. These gapped states are reminiscent of the localized electrons discussed in the literature.<sup>10,11,13,38</sup> At large values of Hund's coupling the itinerant electrons are also gapped at half-filling while keeping a finite density at the Fermi level. We uncover the different role that orbitals play in the stabilization of the orbital ordering and consequently of the  $(\pi, 0)$  antiferromagnetic state. Within a model of localized and itinerant orbitals, we find that while superexchange<sup>20</sup> between  $xy$  and  $yz$  contributes to generate orbital ordering between  $yz$  and  $zx$ , it is necessary to invoke the kinetic energy gain of the itinerant electrons along the ferromagnetic direction to describe the observed features. We analyze this result in connection with the resistivity anisotropy.<sup>26,27</sup> We argue that iron pnictides are close to the boundary between *itinerant* and *strong orbital differentiation* regimes and that it could be possible to cross this boundary with doping.

We consider an interacting two-dimensional five-orbital model for the FeAs layer, as described in Ref. [22]. The Fe orbitals are defined within the one-iron unit cell and hence  $x$  and  $y$  are given by the Fe-Fe nearest neighbor directions. Only local interactions are included. Interactions with rotational symmetry can be expressed in terms of only two parameters: the intra-orbital Hubbard  $U$  and the Hund's coupling  $J_H$ .<sup>39</sup> We focus on the metallic  $(\pi, 0)$  antiferromagnetic state and study the phase diagram as a function of  $U$  and  $J_H/U$  with interactions treated at the Hartree-Fock level.<sup>22</sup>

For the tight-binding we use the model described in Ref. [40] and obtained within the Slater-Koster

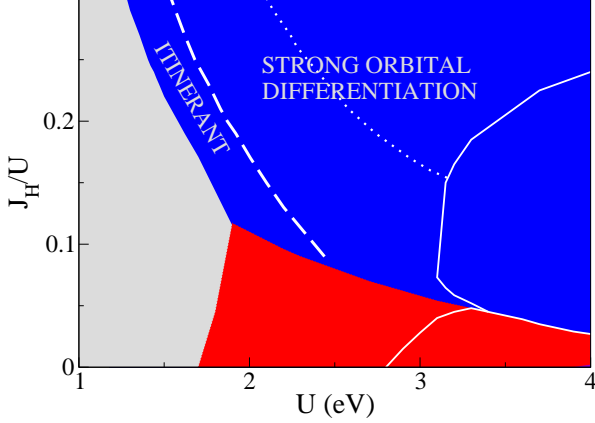


FIG. 1: (Color online) This figure summarizes the main results of this work. The colors distinguish the different  $(\pi, 0)$  magnetic phases of the undoped (6 electrons in 5 d orbitals) system as a function of the local interaction parameters  $U$  and  $J_H$ .<sup>22</sup> The grey area is the non-magnetic region. The blue and red areas are magnetic with a high moment (parallel orbital moments) and a low moment (antiparallel orbital moments) state respectively. The white solid lines on the right separate the metallic ( $U \lesssim 3$ ) from the insulating ( $U \gtrsim 3$ ) state. We have analyzed the orbital differentiation within the blue metallic area. We distinguish two different regions that we label, with increasing  $U$ , as *itinerant* and *strong orbital differentiation*. The strong orbital differentiation region can be further splitted by the opening of a gap at half-filling, see text for discussion.

formalism<sup>41</sup> that takes into account the symmetry of the orbitals and the lattice. In this model the tight-binding parameters are analytic functions of the angle  $\alpha$  formed by the Fe-As bond and the Fe plane. The resulting bands, their orbital compositions, the Fermi surface, and the modifications induced by  $\alpha$  are all consistent with ab-initio calculations.<sup>40</sup> This allows us to straightforwardly explore the effect of the Fe-plane lattice structure on the electronic properties. Except when specifically stated, the results are obtained for the undoped case with six electrons per iron  $n = 6$ , and regular tetrahedra  $\alpha = 35.3^\circ$ .

The main results of our analysis are summarized in Fig. 1 on top of the  $(\pi, 0)$  magnetic phase diagram previously reported in Ref. [22]. The system becomes insulating on the right of the solid white lines. In the grey region the system is not magnetic and the red area corresponds to a low moment state, in which Hund's rule is violated.<sup>22,42–44</sup> The blue high moment state fulfills Hund's rule. Deep in the insulating regime, this state has a spin  $S = 2$  with filled  $x^2 - y^2$  and half-filled  $xy$ ,  $yz$ ,  $zx$ , and  $3z^2 - r^2$  [22]. In the region of larger  $U$ , an increasing  $J_H/U$  leads to metallicity.<sup>45</sup> We focus here on the metallic blue state, on the left of the solid line. Decreasing the value of  $U$  we find different regions which differ on

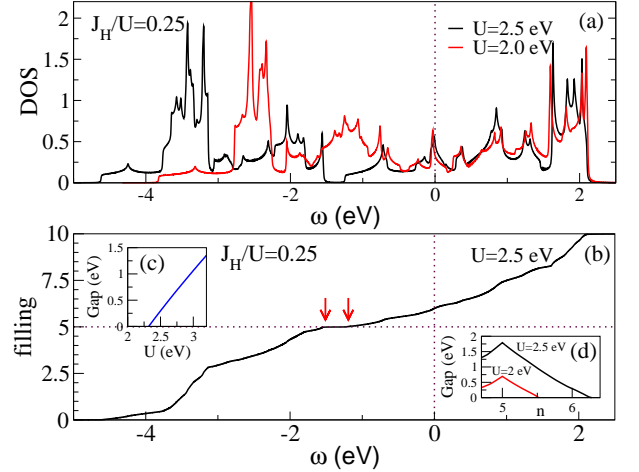


FIG. 2: (Color online) (a) Total density of states for  $J_H/U = 0.25$  and  $U = 2$  eV (red) and  $U = 2.5$  eV (black). The Fermi energy is at  $\omega = 0$ . For  $U = 2.5$  eV, a gap has opened around  $\omega \sim -1.5$  eV, which corresponds to half-filling as illustrated in (b), where the integrated density of states (filling) is shown. This opening of a gap at half-filling in the total density of states characterizes the region on the right of the dotted curve within the *strong orbital differentiation* area in Fig. 1. In contrast, there is no gap for  $U = 2$  eV. (c) Size of the gap at half-filling as a function of  $U$  for  $n = 6$ . (d) Gap as a function of doping  $n$  for the two different values of  $U$ . The gap has a maximum at  $n = 5$ .

their electronic structure and the related orbital differentiation. The regions have been labelled *strong orbital differentiation* and *itinerant*. The nature of the different regions can be inferred from the analysis of the density of states, magnetization and orbital filling curves.

We first focus on the *strong orbital differentiation* region of the phase diagram. Fig. 2 represents the total density of states in two points of this region on both sides of the dotted curve in Fig. 1:  $U = 2$  eV and  $U = 2.5$  eV, both with  $J_H/U = 0.25$  and  $n = 6$ . In both cases, the system is metallic with no gap at the Fermi level. However, the two curves are qualitatively different with a gap clearly showing below the Fermi energy only for the largest value of  $U$ . The opening of this gap in the phase diagram is signaled with a dotted curve in Fig. 1. In Fig. 2(b) it is shown that the gap opens at an energy that corresponds to half-filling (five electrons in the five d orbitals). It increases upon hole doping (decreasing  $n$ ) reaching a maximum at  $n = 5$  (Fig. 2(d)). Once this gap opens, its size depends linearly and much stronger on  $U$  than the splittings at other energies (Fig. 2(c)). This gap was found and discussed on the basis of LDA+ $U$  calculations.<sup>46</sup>

More can be learned about this *strong orbital differentiation* region by looking at the projection of the density of states on the five Fe d orbitals. The integrated density of states (filling) of the orbitals as a function of the energy is shown in Fig. 3 for the same two points of the phase

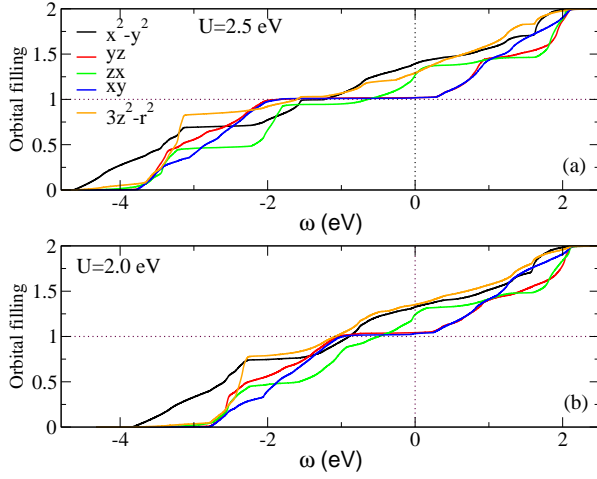


FIG. 3: (Color online) Orbital fillings as a function of energy in the *strong orbital differentiation* regime for (a)  $U = 2.5$  eV and (b)  $U = 2$  eV. For  $U = 2.5$  eV all the orbitals show the gap at negative energies.  $yz$  and  $xy$  are gapped at the Fermi energy while the other three orbitals are gapped only below the Fermi energy. In contrast, for  $U = 2$  eV only two orbitals ( $yz$  and  $xy$ ) show the gap at half-filling while the other three orbitals are itinerant.

diagram as in Fig. 2. The first thing we notice is that for both values of the interaction two orbitals ( $xy$  and  $yz$ ) open a gap at half-filling: their gap is already quite large for  $U = 2$  eV and extends up to the Fermi level. This orbital selective gap is not apparent when looking at the total density of states, Fig. 2. The opening of the gap at negative energies in the total density of states is then related to the appearance of the gap in the other three orbitals  $zx$ ,  $x^2 - y^2$ , and  $3z^2 - r^2$ . However, these three orbitals, unlike  $xy$  and  $yz$ , remain itinerant in this region, with a finite density of states at the Fermi energy. The orbital differentiation just discussed is concomitant with orbital ordering:  $zx$  tends to be more filled and away from half-filling than  $yz$ , which is stuck to half-filling.

Motivated by this orbital differentiation we analyze the stability of magnetism within a model of localized and itinerant orbitals. Assuming localized  $xy$  and itinerant  $x^2 - y^2$  and  $3z^2 - r^2$ , we explore the different tendencies of  $yz$  and  $zx$ . To second order in perturbation theory in the hoppings,  $yz$  ( $zx$ ) has a larger intraorbital exchange along the antiferromagnetic  $x$ -direction (ferromagnetic  $y$ -direction) favoring localization of  $yz$  (delocalization of  $zx$ ) in a magnetic state with  $(\pi, 0)$  ordering.<sup>20</sup> This anisotropic exchange comes from the counter-intuitive hoppings relation  $|t_{yz,yz}^x| > |t_{yz,yz}^y|$  arising from the combination of direct Fe-Fe and indirect Fe-Pn-Fe hopping amplitudes.<sup>40</sup> On the other hand, exchange between  $xy$  and  $yz$  ( $zx$ ) is finite only in the ferromagnetic  $y$ -direction (antiferromagnetic  $x$ -direction) and opposes the localization of  $yz$ . As a consequence, as shown in Fig. 4(b), there is more energy gain due to the localization of  $zx$  than to the localization of  $yz$  for regular tetrahedra ( $\alpha = 35.3^\circ$ ).

For elongated tetrahedra ( $\alpha > 35.3^\circ$ ), the localization of  $zx$  becomes much more advantageous in terms of exchange energy, but this does not affect the sign of the orbital ordering calculated within Hartree-Fock and shown in Fig. 4(a). Moreover, the trend changes for smaller values of  $\alpha$ , where the localization of  $yz$  brings an energy gain, but this is not reflected in the magnitude of the orbital ordering in Fig. 4(a).

A deeper analysis of the orbital dependent hoppings as a function of  $\alpha$  helps to clarify the situation. The hoppings involving  $yz$  and  $zx$  are anisotropic in the plane,<sup>20,40</sup> see Fig. 4(c). Of those, for a regular tetrahedron ( $\alpha = 35.3^\circ$ ), the largest hoppings in absolute value in the  $x$ -direction are  $t_{yz,yz}^x$ ,  $t_{yz,x^2-y^2}^x$ ,  $t_{yz,3z^2-r^2}^x$ , and  $t_{zx,xy}^x$ . By symmetry, simply exchanging  $yz \leftrightarrow zx$ , the largest hoppings in the  $y$ -direction are  $t_{zx,zx}^y$ ,  $t_{zx,x^2-y^2}^y$ ,  $t_{zx,3z^2-r^2}^y$ , and  $t_{yz,xy}^y$ . From these relations, we see that three orbitals ( $zx$ ,  $x^2 - y^2$ , and  $3z^2 - r^2$ ) prefer to be itinerant to gain kinetic energy in the ferromagnetic  $y$ -direction. This gain in kinetic energy is maintained when the tetrahedra are elongated while the localization of  $yz$  would become even more unfavourable in terms of exchange energy. In squeezed tetrahedra the hopping between  $zx$  and  $3z^2 - r^2$  along the  $y$ -direction strongly decreases and induces a reduction of the orbital ordering. Within this model, the orbital ordering, which does not change sign for the experimentally relevant values of  $\alpha$ , see Fig. 4(a), arises due to the interplay of the exchange energy in the  $x$ -direction due to  $yz$  localization and the kinetic energy in the  $y$ -direction due to the itinerancy of  $zx$ ,  $x^2 - y^2$ , and  $3z^2 - r^2$ . Depending on  $\alpha$ , these two factors cooperate (squeezed tetrahedra) or compete (regular or elongated tetrahedra), with an overall dominance of the kinetic energy gain. Therefore, this kinetic energy gain is important to stabilize the  $(\pi, 0)$  magnetic ordering in the orbital differentiation regime.

The orbital differentiation sustained by the gain in kinetic energy in the  $y$ -direction survives upon doping, as shown in Fig. 5. With decreasing  $n$  (hole-doping)  $zx$  filling decreases fast, changing the sign of the orbital ordering at some point but, remarkably, it is kept away from half-filling, together with  $3z^2 - r^2$ , even at  $n = 5$ .<sup>48</sup>

So far, we have discussed the nature of the *strong orbital differentiation* region of the phase diagram in Fig. 1. If we go on decreasing  $U$ , the orbital differentiation features get weaker, with  $xy$  and  $yz$  getting a finite density of states at the Fermi level, and all carriers are itinerant.

In Fig. 6 (a) the magnetization is depicted as a function of  $U$  (black curve) while the evolution of the orbital fillings and their derivatives with  $U$  are shown in (b) and (c) respectively. For the values of  $U$  with strong orbital differentiation the magnetization has the typical concave shape, but for smaller values of  $U$ , the shape of the curve is more complex.  $xy$  and  $yz$  orbitals are shown to go to half-filling at around the same value  $U^*$  of the interactions at which the magnetization becomes concave. Therefore, we estimate the value of  $U^*$ , which separates the itinerant and strong orbital differentiation regimes in



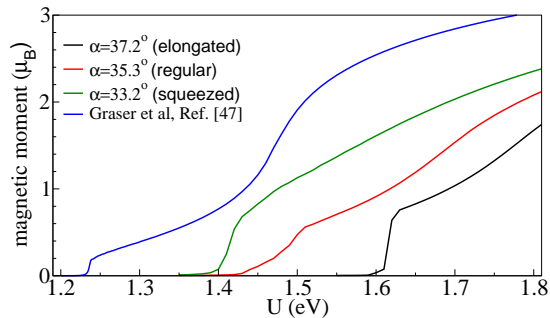


FIG. 7: (Color online) Magnetization versus  $U$  for  $J_H/U = 0.25$  for different values of the angle  $\alpha$  formed by the Fe-As bond with the Fe plane, and for a different tight-binding model reported in Ref. [47]. For sufficiently high values of  $U$ , the magnetization recovers a typical concave shape while for the smaller values of  $U$  the curves have different shapes.

in particular on the presence or absence of a hole Fermi pocket at  $(\pi, \pi)$ . To illustrate this, we show in Fig. 7 the dependence of the magnetization on  $U$  for our model<sup>40</sup> with different values of  $\alpha$ , all with a hole Fermi pocket at  $(\pi, \pi)$ , and for a different tight-binding model<sup>47</sup> that presents no such Fermi pocket. The Fermi surfaces for these different cases can be found in Refs. [40] and [47], respectively. While both the value of  $U$  at which magnetism appears and  $U^*$  depend slightly on the model under consideration, the description presented here in terms of itinerant and strong orbital differentiation regimes is valid in all these cases. Moreover the value of the magnetic moment at the crossover is similar for all these models.

The doping dependence of  $U^*$  is shown in the inset of Fig. 6 (a). Its value decreases (increases) upon hole (electron) doping monotonously. This is in contrast with the value of the interaction at which antiferromagnetism appears  $U_{mag}$ . The different dependence on doping of  $U_{mag}$  and  $U^*$  gives support to the existence of two regimes: itinerant and strong orbital differentiation. Starting with  $n = 6$  in the itinerant region and doping with holes the system can either enter in the magnetic orbital differentiation region or lose magnetism, depending on the value of  $U$ . Note that with hole doping  $(\pi, \pi)$  correlations start to dominate over  $(\pi, 0)$ ,<sup>45</sup> possibly affecting the stability of magnetism.

In conclusion, we have found that except for small values of the interactions close to the non magnetic boundary, the metallic  $(\pi, 0)$  antiferromagnetic state satisfying Hund's rule is characterized by a strong orbital differentiation between half-filled  $xy$  and  $yz$  orbitals, showing a large gap at the Fermi level and itinerant  $zx$ ,  $3z^2 - r^2$  and  $x^2 - y^2$  orbitals away from half-filling and showing a finite density of states at the Fermi level.

The large gap at the Fermi level shown by the half-filled orbitals suggests a connection to localization. The present approach cannot address such localization but we believe that it will appear in more elaborate calcu-

lations. Within this interpretation, the larger tendency to localization of  $xy$  agrees with it being close to half-filling in the non-interacting bands and thus very sensitive to interactions, while  $3z^2 - r^2$  and  $x^2 - y^2$  have the largest filling and thus more itinerant behavior. This result is consistent with DMFT and slave-spin calculations in the paramagnetic state.<sup>1,16-18,38,49</sup> The selective localization of  $xy$  orbital could have been observed already in ARPES measurements on the 122 selenides in the paramagnetic state.<sup>38</sup> Our calculations also uncover a strong orbital differentiation between  $yz$  and  $zx$  in the antiferromagnetic state where the tetragonal symmetry is broken. We hope our results encourage new polarized ARPES measurements in the  $(\pi, 0)$  magnetic state.

In a previous work, we found orbital ordering to promote a larger conductivity in the ferromagnetic direction except in a striped region of the phase diagram close to the magnetic transition (see Fig. 1(b) in Ref.[26]). This is consistent with the stabilization of the  $(\pi, 0)$  magnetic state driven by itinerancy in the  $y$ -direction (and the concomitant orbital order) in the region of the phase diagram with both itinerant and gapped carriers.

Current estimates for the interactions<sup>50</sup> situate the iron superconductors close to the boundary between the *itinerant* and the *strong orbital differentiation* regimes. This is in accord with the values of the magnetic moment that we obtain in this region, expected in our approximation to be similar to those found in LDA calculations.<sup>5</sup> Moreover, the anisotropy of the conductivity found experimentally in the 122 compounds,<sup>24,25</sup> which is such that the conductivity is larger in the antiferromagnetic direction, is consistent with the system not being very deep in the orbital differentiated regime, where the opposite sign of the anisotropy has been calculated.<sup>26</sup> The exact position in the phase diagram could be different among families.

Finally, the boundary between the *itinerant* and the *strong orbital differentiation* regimes shifts to lower (larger) values of the interaction with hole (electron) doping. Electron doping promotes itinerancy while hole-doping can induce selective orbital localization. Therefore, by changing the doping it could be possible to cross this boundary and enter a different regime. This is consistent with recent DMFT calculations<sup>51</sup> in FeSe in the non-magnetic state which show a selective Mott transition of the  $xy$  orbital with hole doping. Slave-spin calculations in 122 selenides also show that the critical  $U$  for the  $xy$  selective Mott transition increases with electron doping.<sup>38,49</sup> In  $\text{KFe}_2\text{As}_2$ , the  $xy$  orbital shows a mass enhancement  $\sim 10$ , much larger than in undoped 122 pnictides.<sup>14</sup> A change in the sign of the resistivity anisotropy in the magnetic state with hole doping has been recently reported.<sup>37</sup> Whether this is caused by hole-doping induced orbital differentiation is at present not known.

We have benefited from conversations with A. Millis, L. Boeri, I. Eremin, M. Capone, L. de Medici, and W. Ku. We acknowledge funding from MINECO-

- 
- \* Electronic address: leni.bascones@icmm.csic.es  
† Electronic address: belenv@icmm.csic.es  
‡ Electronic address: calderon@icmm.csic.es
- <sup>1</sup> H. Ishida and A. Liebsch, Phys. Rev. B **81**, 054513 (2010).
  - <sup>2</sup> P. Werner, M. Casula, T. Miyake, F. Aryasetiawan, A. J. Millis, and S. Biermann, Nature Physics **8**, 331 (2012).
  - <sup>3</sup> T. Misawa, K. Nakamura, and M. Imada, Phys. Rev. Lett. **108**, 177007 (2012).
  - <sup>4</sup> S. Raghu, X. Qi, C.-X. Liu, D. Scalapino, and S.-C. Zhang, Phys. Rev. B **77**, 220503 (2008).
  - <sup>5</sup> I. Mazin, M. D. Johannes, L. Boeri, and D. S. K. Koepf, Phys. Rev. B **78**, 085104 (2008).
  - <sup>6</sup> A. Chubukov, D. Efremov, and I. Eremin, Phys. Rev. B **78**, 134512 (2008).
  - <sup>7</sup> V. Cvetkovic and Z. Tesařovic, Europhysics Lett. **85**, 37002 (2009).
  - <sup>8</sup> T. Yildirim, Physical Review Letters **101**, 057010 (2008).
  - <sup>9</sup> Q. Si and E. Abrahams, Phys. Rev. Lett. **101**, 076401 (2008).
  - <sup>10</sup> J. Wu, P. Phillips, and A. H. Castro Neto, Phys. Rev. Lett. **101**, 126401 (2008).
  - <sup>11</sup> L. de' Medici, S. R. Hassan, and M. Capone, Journal of Superconductivity and Novel Magnetism **22**, 535 (2009).
  - <sup>12</sup> W. Lv, F. Krüger, and P. Phillips, Phys. Rev. B **82**, 045125 (2010).
  - <sup>13</sup> W.-G. Yin, C.-C. Lee, and W. Ku, Physical Review Letters **105**, 107004 (2010).
  - <sup>14</sup> T. Yoshida, S. Ideta, I. Nishi, A. Fujimori, M. Yi, R. G. Moore, S. K. Mo, D.-H. Lu, Z.-X. Shen, Z. Hussain, et al. (2012), arXiv:1205.6911.
  - <sup>15</sup> T. Sudayama, Y. Wakisaka, T. Mizokawa, S. Ibuka, R. Morinaga, T. J. Sato, M. Arita, H. Namatame, M. Taniguchi, and N. Saini (2012), arXiv:1206.2985.
  - <sup>16</sup> M. Aichhorn, S. Biermann, T. Miyake, A. Georges, and M. Imada, Phys. Rev. B **82**, 064504 (2010).
  - <sup>17</sup> Z. P. Yin, K. Haule, and G. Kotliar, Nature Physics **7**, 294 (2010).
  - <sup>18</sup> R. Yu and Q. Si, Phys. Rev. B **86**, 085104 (2012).
  - <sup>19</sup> W. Lv, J. Wu, and P. Phillips, Phys. Rev. B **80**, 224506 (2009).
  - <sup>20</sup> C.-C. Lee, W.-G. Yin, and W. Ku, Phys. Rev. Lett. **103**, 267001 (2009).
  - <sup>21</sup> F. Krüger, S. Kumar, J. Zaanen, and J. van den Brink, Phys. Rev. B **79**, 054504 (2009).
  - <sup>22</sup> E. Bascones, M. J. Calderón, and B. Valenzuela, Phys. Rev. Lett. **104**, 227201 (2010).
  - <sup>23</sup> M. Daghofer, Q.-L. Luo, R. Yu, D. X. Yao, A. Moreo, and E. Dagotto, Phys. Rev. B **81**, 180514 (2010).
  - <sup>24</sup> J.-H. Chu, J. G. Analytis, D. Press, K. De Greve, T. D. Ladd, Y. Yamamoto, and I. R. Fisher, Phys. Rev. B **81**, 214502 (2010).
  - <sup>25</sup> M. A. Tanatar, E. C. Blomberg, A. Kreyssig, M. G. Kim, N. Ni, A. Thaler, S. L. Bud'ko, P. C. Canfield, A. I. Goldman, I. I. Mazin, et al., Phys. Rev. B **81**, 184508 (2010).
  - <sup>26</sup> B. Valenzuela, E. Bascones, and M. J. Calderón, Phys. Rev. Lett. **105**, 207202 (2010).
  - <sup>27</sup> C.-C. Chen, J. Maciejko, A. P. Sorini, B. Moritz, R. R. P. Singh, and T. P. Devereaux, Phys. Rev. B **82**, 100504 (2010).
  - <sup>28</sup> A. Dusza, A. Lucarelli, F. Pfüner, J.-H. Chu, I. Fisher, and L. Degiorgi, Europhys. Lett. **93**, 37002 (2011).
  - <sup>29</sup> J. Zhao, D. T. Adroja, D.-X. Yao, R. Bewley, S. Li, X. F. Wang, G. Wu, X. H. Chen, J. Hu, and P. Dai, Nature Physics **5**, 555 (2009).
  - <sup>30</sup> R. R. P. Singh, arXiv:0903.4408 (2009).
  - <sup>31</sup> T. Shimojima, K. Ishizaka, Y. Ishida, N. Katayama, K. Ohgushi, T. Kiss, M. Okawa, T. Togashi, X. Y. Wang, C. T. Chen, et al., Phys. Rev. Lett. **104**, 057002 (2010).
  - <sup>32</sup> T.-M. Chuang, M. P. Allan, J. Lee, Y. Xie, N. Ni, S. L. Bud'ko, G. S. Boebinger, P. C. Canfield, and J. C. Davis, Science **327**, 181 (2010).
  - <sup>33</sup> M. Nakajima, T. Liang, S. Ishida, Y. Tomioka, K. Kihou, C. H. Lee, A. Iyo, H. Eisaki, T. Kakeshita, T. Ito, et al., PNAS **108**, 12238 (2011).
  - <sup>34</sup> W. Lv and P. Phillips, Phys. Rev. B **84**, 174512 (2011).
  - <sup>35</sup> R. M. Fernandes, E. Abrahams, and J. Schmalian, Phys. Rev. Lett. **107**, 217002 (2011).
  - <sup>36</sup> I. R. Fisher, L. Degiorgi, and Z. X. Shen, Rep. Prog. Phys. **74**, 124506 (2011).
  - <sup>37</sup> E. C. Blomberg, M. A. Tanatar, R. M. Fernandes, B. Shen, H.-H. Wen, J. Schmalian, and R. Prozorov (2012), arXiv:1202.4430.
  - <sup>38</sup> M. Yi, D. Lu, R. Yu, S. Riggs, J.-H. Chu, B. Lv, Z. Liu, M. Lu, Y. Cui, M. Hashimoto, et al. (2012), arXiv:1208.5192.
  - <sup>39</sup> C. Castellani, C. R. Natoli, and J. Ranninger, Phys. Rev. B **18**, 4945 (1978).
  - <sup>40</sup> M. J. Calderón, B. Valenzuela, and E. Bascones, Phys. Rev. B **80**, 094531 (2009).
  - <sup>41</sup> J. Slater and G. Koster, Phys. Rev. **94**, 1498 (1954).
  - <sup>42</sup> F. Cricchio, O. Granas, and L. Nordstrom, Phys. Rev. B **81**, 140403 (2009).
  - <sup>43</sup> G.-Q. Liu, arXiv:1105.5412v1 (2011).
  - <sup>44</sup> T. Schikling, F. Gebhard, and J. Bünemann, Phys. Rev. Lett. **106**, 146402 (2011).
  - <sup>45</sup> M. J. Calderón, G. León, B. Valenzuela, and E. Bascones, Phys. Rev. B **86**, 104514 (2012).
  - <sup>46</sup> W.-G. Yin, C.-H. Lin, and W. Ku, Phys. Rev. B **86**, 081106 (R) (2012).
  - <sup>47</sup> S. Graser, T. Maier, P. Hirschfeld, and D. Scalapino, New J. Phys. **11**, 025016 (2009).
  - <sup>48</sup> Note that this is a consequence of the imposed  $(\pi, 0)$  ordering. In fact, a  $(\pi, \pi)$  checkerboard magnetic order is stabilized when heavily doping with holes towards  $n = 5$ . See Ref.[45].
  - <sup>49</sup> R. Yu and Q. Si (2012), arxiv:1208.5547.
  - <sup>50</sup> T. Miyake, K. Nakamura, R. Arita, and M. Imada, J. Phys. Soc. Jpn. **79**, 044705 (2010).
  - <sup>51</sup> L. de' Medici, G. Giovannetti, and M. Capone (2012), unpublished.